

Topological Defects and Morphology of Graphitic Carbon Materials: An Approach Based on Differential Geometry

Masahiko HAYASHI*

*Graduate School of Information Sciences, Tohoku University
Aramaki, Aoba-ku, Sendai 980-8579, Japan*

(Received February 17, 2018)

It has been known that pentagons and heptagons in hexagonal graphitic network give rise to a certain amount of curvature in the three dimensional structure of graphitic carbon materials. The amount of curvature is quantized due to the symmetry of graphite and, as a result, the structure formed by the network is also restricted. We clarify the effects of curvature quantization on the forms of graphitic carbon materials, employing the knowledge of differential geometry, especially the Gauss-Bonnet theorem.

KEYWORDS: nanotube, fullerene, graphite, topological crystal, disclination, differential geometry

1. Introduction

After the discovery of Fullerenes¹⁻⁵⁾ and nanotubes,⁶⁾ graphitic carbon materials have been studied intensively. Until now many intriguing structures have been discovered: larger Fullerenes,^{7,8)} nanohorns,⁹⁾ kinked nanotubes,^{10,11)} Y-junctions^{11,12)} and so on. The discovery of these materials has been stimulated interests in more exotic structures, such as negatively curved periodic minimal surface.¹³⁻¹⁵⁾

From the very beginning of the research of these materials, the geometrical methods have been powerful tools to predict, investigate and clarify the new structures of graphitic carbon materials. For example, based on the Euler's formula, Iijima was able to guess one of the basic characters of Fullerene, *i.e.*, the existence of twelve pentagons (five-membered rings), before the clarification of the C₆₀ structure.³⁾

In this paper, aiming to apply the method of differential geometry to the analysis of more complicated topologically nontrivial structures, we develop a simple geometrical model for the graphitic carbon materials. Basic point of our model is the assumption that the graphite sheet is free from expansion and contraction; it can only be bent without changing the area of any part of the sheet. In order to understand this, one can imagine a sheet of ordinary paper, where expansion or contraction is much more difficult than bending. Mathematically, this kind of surface is called *developable surface*; when a part of the surface is cut out, it can be developable on a plane without expansion or contraction. For example, the side of a cylinder or a cone is a developable surface, whereas a part of a sphere is not. Whether a surface is really "curved" like spheres or is just a bent plane like sides of cylinders or cones is distinguished by introducing the so-called *Gaussian curvature* in the framework of the differential geometry (see text for details). In the case of graphitic carbon materials, non-zero Gaussian curvature arises only from the *disclinations*, which correspond to the pentagons and heptagons in the graphitic network. The Gaussian curvature caused by the disclinations is

quantized due to the hexagonal symmetry of the graphite sheet and the possible forms of the graphitic carbon materials are restricted by this effect. The main part of this paper is therefore devoted to the investigation of the relation between the quantized Gaussian curvature and the structures of the graphitic carbon materials for several simple cases, such as cones, spheres, kinked tubes and so on.

Here we would like to note that today the crystals with topologically interesting forms are not limited to the graphitic carbon materials. Recently, "nanotubes" are found in several other materials, such as MoS₂,¹⁶⁾ MgB₂ and NbSe₂.¹⁷⁾ Rings and Möbius strip-type crystals are also found for NbSe₃.¹⁸⁾ These facts suggest that "topological crystals" are commoner than we expect. We believe that the present approach will also shed a new light on these new materials in the future.

This paper is organized as follows: in Sec.2, we describe the basic properties of the disclinations in graphite sheet and show how the Gaussian curvature per one disclination is quantized. In Sec.3, we apply the Gauss-Bonnet theorem to the cases of Fullerenes, Cones, kinked tubes and so on, and clarify how the quantized Gaussian curvature affects the structure of the graphitic carbon materials. In Sec.4, we give some discussion on the experimental observation of the prediction of this paper. The possible development of our treatment is also discussed. In Sec.5, we summarize our results. In Appendices, we introduce the basic framework of the differential geometry, which is employed in this paper.

2. Disclination in Graphitic Network

First we introduce the basic assumption of our model. Generally, the graphite sheet is hard against expansion and contraction, since the *sp*² bonding of carbon is strong and the bond length is almost fixed. The shear deformation is also suppressed due to the firmly fixed bond angle. Therefore the deformation allowed for a graphite sheet is only the bending without changing the area of any part of the graphitic network. This means, from the knowledge of the differential geometry, that the graphite sheet forms a developable surface or, equivalently, the Gaussian cur-

* hayashi@cmt.is.tohoku.ac.jp

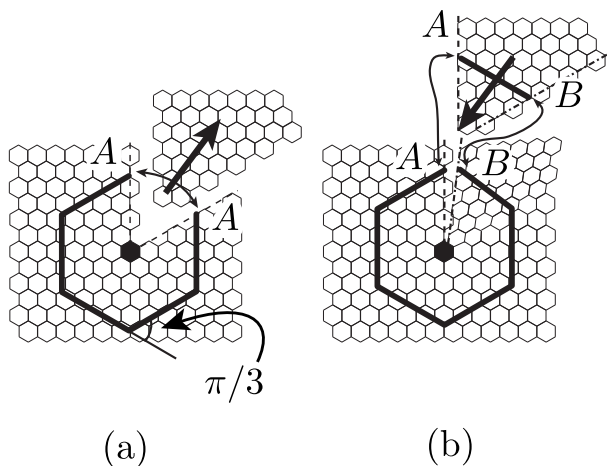


Fig. 1. (a) Formation of a $\pi/3$ wedge disclination and (b) a $-\pi/3$ wedge disclination. (a) Geodesic polygon around a $\pi/3$ disclination, and (b) that around a $-\pi/3$ disclination are also shown with bold lines. The points marked with A's and B's should be merged in each figure, so that the bold lines are closed.

vature K of the graphite sheet vanishes (see Appendix for more details). If we employ a more easy analogy, the graphite sheet is like a sheet of ordinary paper; in contrast to a rubber sheet, expanding or contracting a sheet of paper is hard, although bending is easy.

The Gaussian curvature is generated in the graphitic network only by introducing disclinations. Disclination is a topological defect created in the following way: At the center of a hexagon of a graphite sheet, there is a six-fold symmetry. Now we cut off one of the six equivalent fan-shaped regions as shown in Fig. 1(a) and join the two edges created by cutting. This operation leaves a pentagon at the center. The structure obtained in this way is called $\pi/3$ wedge disclination. If we cut off two of the fan-shaped regions, we obtain $2\pi/3$ wedge disclination. In this case, there is a square at the center. Usually a $2\pi/3$ wedge disclination has much higher energy than a $\pi/3$ wedge disclination and is almost negligible. (Instead of a $2\pi/3$ wedge disclination, we may introduce two $\pi/3$ ones at some distance from each other.) On the other hand, if we add one extra fan-shaped region as shown in Fig. 1(b), the obtained structure is $-\pi/3$ wedge disclination, which has a heptagon at the center. In this case also, octagons are less favored than heptagons. From now on we use the word “disclination” instead of “wedge disclination” for short.

Next we calculate the Gaussian curvature generated by a disclination. Here we consider only one disclination in a graphite sheet. The Gaussian curvature of the disclination is calculated from the Gauss-Bonnet theorem,

$$\iint_D K dA = 2\pi - \sum_{i=1}^N \theta_i, \quad (1)$$

where D is the region surrounded by a geodesic polygon on the surface (graphite sheet), which is shown in Fig. 1 by bold lines, and the l.h.s. is the surface integral of the Gaussian curvature K over the region D . In the present case, K is non-zero only at the center where

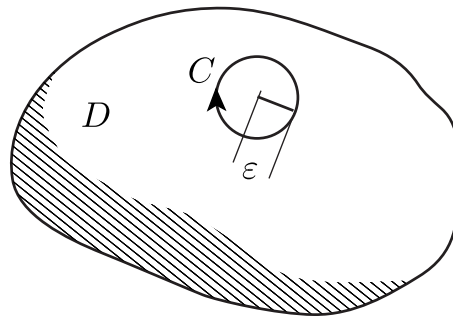


Fig. 2. A simply connected closed surface. C is a small circle on the surface and D is the region outside of the circle C .

the disclination is located. θ_i is the angle between the neighboring sides of the polygon (exterior angles) at the i -th vertex (See Appendix B.1 for details.) We can easily see from Fig. 1 (a) that the r.h.s. of Eq. (1) reads $2\pi - 5\pi/3 = \pi/3$. Therefore the Gaussian curvature generated by a $\pi/3$ disclination is $\pi/3$. In the same way, the Gaussian curvature generated by a $-\pi/3$ disclination is $-\pi/3$, by considering the geodesic polygon as shown in Fig. 1 (b).

3. Gauss-Bonnet theorem and its application to various graphitic carbon materials

3.1 Fullerenes

Fullerenes are simply connected closed surface formed by a graphite sheet. Here we calculate the total curvature of the closed surface using the Gauss-Bonnet theorem. We consider the surface as depicted in Fig. 2 and draw a small circle C with radius ε on it. The circle is so small that the surface in the circle can be regarded as a plane. The region D in this case is the outside of the small circle.

We apply the Gauss-Bonnet theorem,

$$\int_C \kappa_g ds + \iint_D K dA = 2\pi, \quad (2)$$

where κ_g is the geodesic curvature of C (see Eq. (B-2) of Appendix B). The geodesic curvature of the circle coincides with the curvature of the circle, as one can see from the definition of the geodesic curvature given in Appendix B.1, and we obtain $\kappa_g = -1/\varepsilon$ (Note that the minus sign comes from the fact that the inside of the circle is the outside of the region D). Then the first term of Eq. (2) equals $2\pi\varepsilon \times (-1/\varepsilon) = -2\pi$ and we obtain

$$\iint_D K dA = 4\pi. \quad (3)$$

This result does not depend on the details of the surface if the surface is a simply connected closed one. In the limit of $\varepsilon \rightarrow 0$, D covers the whole region of the surface.

Since the Gaussian curvature per a $\pi/3$ disclination is $\pi/3$, twelve $\pi/3$ disclinations are required to make a graphite sheet closed. This means that there are always twelve pentagons on a simply connected closed graphitic carbon material, which is a well-known result for Fullerenes.

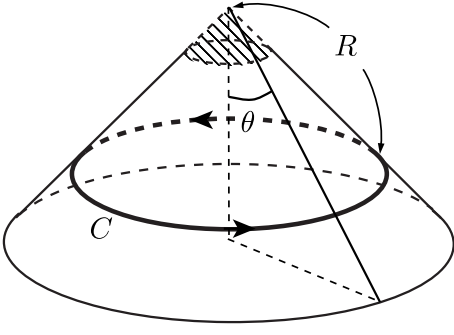


Fig. 3. A circular cone. Disclinations are located in the shaded region. C is a circle on the cone whose distance from the vertex is R . θ is the angle between the generating line and the center line of the cone.

3.2 Cones

Next we consider the circular cone-shaped graphitic carbon material as depicted in Fig. 3. Here we consider a circle C on the cone as shown in Fig. 3, where the distance from the vertex of the cone to the circle is R . The geodesic curvature of C is estimated by developing the side of the cone on a plane. The curve C , when developed on a plane, becomes a circle of radius R . Therefore its curvature, $1/R$, gives the geodesic curvature of C on the cone. (Note that the geodesic curvature of a curve on a developable surface is obtained by developing the surface on a plane and measuring the curvature of the curve.) Integrating the geodesic curvature along the circle, we obtain $2\pi R \sin\theta \times (1/R)$, where θ is the angle between the generating line and the center line of the cone. From Eq. (2) we obtain the Gaussian curvature inside of the curve C as

$$\iint_D K dA = 2\pi(1 - \sin\theta). \quad (4)$$

This curvature is generated by the disclinations existing in the shaded region of the cone in Fig. 3. Therefore it should be quantized in the unit of $\pi/3$. If we assume that the total number of disclinations (the number of $\pi/3$ disclinations minus that of $-\pi/3$ disclinations) is n , we obtain $\theta = \theta_n$, where

$$\theta_n = \arcsin\left(1 - \frac{n}{6}\right). \quad (5)$$

Here we assume that n is positive (see Discussion for the case of negative n). In order that $0 < \theta_n < \pi/2$, n is limited as $1 \leq n \leq 5$ and we obtain $\theta_1 = 56.4^\circ$, $\theta_2 = 41.8^\circ$, $\theta_3 = 30^\circ$, $\theta_4 = 19.5^\circ$ and $\theta_5 = 9.6^\circ$ (in degree). In case of $n = 6$, we have a tube in the limit of an infinitely sharp cone.

The results obtained until now are rather trivial ones, which are also obtained in terms of more elementary arguments. In the next section we see a little more non-trivial cases.

3.3 Kinked nanotube

Here we consider a kinked nanotube. If there are several $\pi/3$ disclinations on one side of a tube and the same number of $-\pi/3$ disclinations on the other side, the tube

has a kink structure, as depicted in Fig. 4(a). We denote the corner angle of the kink by Θ . We assume that the negative (positive) disclinations are located in the shaded region (the region behind the tube not depicted here) and except for these regions the surface is free from the Gaussian curvature ($K = 0$).¹⁹⁾ Now we consider a curve $C = C_1 + C_2 + C_3 + C_4$ in Fig. 4(a). The region surrounded by C is denoted by D . C_2 and C_4 are perpendicular to the axis of the tube and comprise geodesic curves.

Next we look at the curves C_1 and C_3 . Here we assume a very simple situation: C_1 and C_3 are the top line and the bottom line of the tube, respectively and are plane curves, namely each curve is included in a single plane. The planes are the tangent planes of the tube. This can be applied to the case that the tube does not change its radius at the kink. The deviation from this situation is also discussed later in this section.

Under the above assumption, we now apply the Gauss-Bonnet theorem to the kinked tube. Since C_1 and C_3 lie in a tangent plane of the tube, at any points on these curves the normal curvature κ_n vanishes. Therefore the curvature of the curve coincides with the geodesic curvature. (See Appendix B.1.)

Then we apply the Gauss-Bonnet theorem to the curve C and the region D . Here we use the following form

$$\int_{C'} \kappa_g ds + \iint_D K dA = 2\pi - \sum_{i=1}^N \theta_i, \quad (6)$$

(see Appendix B.2). C' means that the integral of κ_g is performed except for the vertex points. Here θ_i is the exterior angle at the vertex i of the line C . On C_2 and C_4 the first term vanishes since they are geodesic curves. On C_1 and C_3 the geodesic curvature coincides with the curvature of the curves. Since C_1 and C_3 are plane curves, their curvature κ is given by $\kappa = d\theta(s)/ds$, where $\theta(s)$ is the angle between the tangent line of the curve and a certain standard line on the plane with s being the length measured along the line. We set the sign of $\theta(s)$ so that it increases when the curve is convex as viewed from the inside of the region D .

Let us calculate the geodesic curvature of C_1 . Using the parameter s along C_1 , the curvature of C_1 is given by $d\theta/ds$ and it gives the geodesic curvature of C_1 . Therefore we can evaluate the first term of Eq. (6) as

$$\int_{C_1} \kappa_g ds = \int_0^l \frac{d\theta}{ds} ds = \theta(l) - \theta(0) = \Theta, \quad (7)$$

where l is the length of C_1 and $s = 0$ corresponds to the starting point of C_1 . C_3 also gives the same contribution.

Noting that the exterior angles between C_1 and C_2 , C_2 and C_3 , C_3 and C_4 , and C_4 and C_1 are all $\pi/2$, we can calculate the Gaussian curvature as

$$\iint_D K dA = -2\Theta. \quad (8)$$

If we set D so that it covers the outer half of the tube

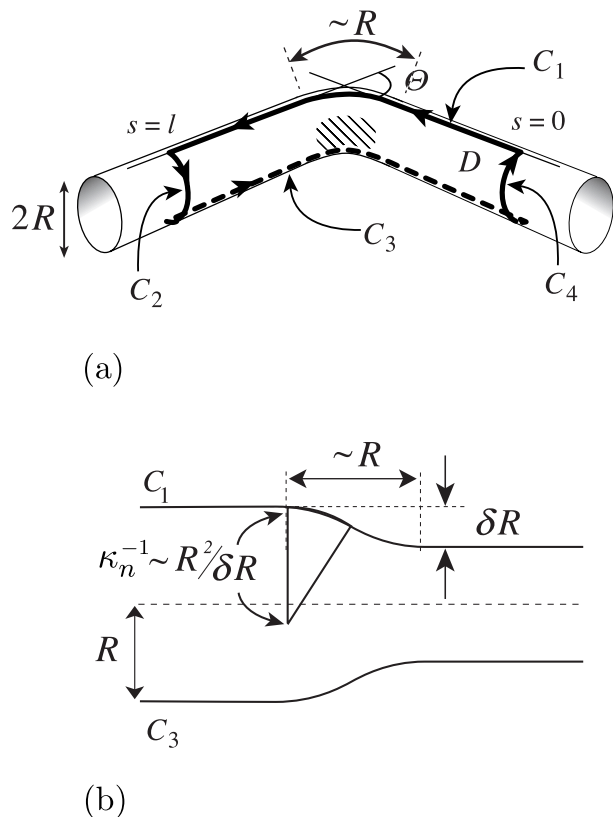


Fig. 4. (a) A kinked tube. Some negative disclinations are expected in the shaded region and the same number of positive ones on the other side. Except for the vicinity of the disclinations, the surface is assumed to be free from Gaussian curvature, *i.e.*, $K = 0$. D is the region on the surface surrounded by $C = C_1 + C_2 + C_3 + C_4$. C_2 and C_4 are perpendicular to the axis of the tube. C_1 (C_3) is the line on the upper (lower) part of the tube. In this figure the tube does not change its radius at the kink position. (b) Cross section of a tube in case that the tube changes its radius near the kink position. The cross section is along the curves C_1 and C_3 . The radius of the curvature near the kink is estimated to be $\sim R^2/\delta R$ from this figure, which corresponds approximately to the normal curvature κ_n of the curve C_1 and C_3 .

(opposite side with the above D), we have the result

$$\iint_D K dA = 2\Theta. \quad (9)$$

Since the Gaussian curvature is quantized in the unit of $\pi/3$ as is mentioned before, Θ can take only the discrete values, multiples of $\pi/6$. This is the most important result of this paper.

Now we consider what happens if the curves C_1 and C_3 are not plane curves. For example, when the tube changes its radius at the kink, this situation appears. In this case, however, there is no simple way to calculate the first term of Eq. (6). Therefore we give a rough estimation of the deviation from the result obtained in Eq. (7).

We consider the case that the tube changes its radius from R to $R + \delta R$ near the kink position. It is expected that the length scale needed for this change is probably of the order of R , which is also the size of the kink region (the transition region from one straight tube to the other). Therefore in this case we expect that C_1 changes

as shown in Fig. 4(b), in which the cross section of the tube along the curves, C_1 and C_3 , is shown. Assuming that C_1 and C_3 interpolate smoothly between two parallel lines outside of the kink, as shown in Fig. 4(b), let us estimate the change of the first term of Eq. (6). Here we limit ourselves to the case of C_1 . The case of C_3 is similar. First we rewrite κ_g in terms of the normal curvature κ_n and the curvature of the curve κ (see Appendix B.1 for the definitions of κ_n),

$$\kappa_g = \sqrt{\kappa^2 - \kappa_n^2}.$$

(We assumed that κ_g has a definite sign in the kink region.) Note that κ_g and κ are the same order $\sim \Theta/R$, since the length of the kink region is roughly $\sim R$ as one can see from Fig. 4(a), and the line integral of κ along the kink region is of the order of Θ . On the other hand, κ_n is much smaller. We estimate κ_n generated by the radius change to be of the order of $\sim \delta R/R^2$ as seen in Fig. 4(b). We now obtain

$$\begin{aligned} \int_{C_1} \kappa_g ds &= \int_{C_1} \sqrt{\kappa^2 - \kappa_n^2} ds \\ &\simeq \Theta + \mathcal{O}\left(\frac{\delta R}{R}\right)^2. \end{aligned} \quad (10)$$

We see that, even if the change of the radius at the kink is about 10%, the correction to the present evaluation is a few percent, which is not too large to spoil the quantization of Θ .²⁰⁾

3.4 Y-junction and other forms with branches

Recently more intriguing structures of graphitic carbon materials are created, including Y-junctions.^{21–27)} Here we describe a general properties derived from the Gauss-Bonnet theorem. Let us consider a graphitic carbon material depicted in Fig. 5. The details of the structure is not important. We denote the number of the branches (tubes) going out of the structure by N .

We note that we can make this structure a closed one by putting half of spherical Fullerenes (caps) to all the ends of the branches. In that case, the number of the disclinations is increased by $6N$, since there are six in each cap.

Here we employ a more general form of the Gauss-Bonnet theorem for closed surfaces (see Appendix B.2 for more details),

$$\iint_S K dA = 4\pi(1 - g), \quad (11)$$

where g is the genus of the surface, which is zero for a simply connected closed surface like a sphere, and one for a torus. In case of Fig. 5, g equals two.

Now we can estimate the number of disclinations in the original structure without caps. Since the integrated gaussian curvature of the capped surface is $4\pi(1 - g)$, there should be $12(1 - g)$ disclinations in total. Among them, $6N$ disclinations come from the caps. Therefore the number of disclinations in the original structure is $12(1 - g) - 6N$.

In case of a Y-junction, $g = 0$ and $N = 3$, and we see



Fig. 5. Graphitic carbon material with several branches of nanotubes. The important feature is the number of the branches (3 in this case) and the genus of the “body” (2 in this case).

that the total number of disclinations is -6 . This means that there are six $-\pi/3$ disclinations, which is consistent with the structure of graphitic carbon material given in Ref. 21.

4. Discussion and Further Problems

The most non-trivial result in this paper is that the corner angle of the kinked nanotube is quantized by $\pi/6$. Although there can be a small deviation in real systems, it is estimated to be small. Now we discuss how this nature of the nanotube is observed in actual experiments. The forms of nanotubes are observed by using the transmission electron microscope. However, in actually synthesized materials, nanotubes are quite randomly piled as seen in Ref. 6. In such a situation, each tube undergoes stress from other tubes and is elastically deformed. Since such deformation is not taken into account in our study, the prediction of this paper does not seem to be easily realized in realistic materials. In order to overcome this difficulty one may try the following two methods. Firstly, if a material can be well separated from other materials and examined individually, the prediction in this paper is easily ascertained. This kind of methods may be done by using the developed nanotechnology in the future. Secondly, one may adopt statistical way to examine the forms of carbon materials. Since the most stable forms of graphitic carbon materials are those predicted in this paper, these forms are more easily realized than the elastically deformed ones. Therefore, in case of the kinked tubes, for example, if one gather data of the kink angles for many kinked tubes and plot the number of kinks as a function of the kink angle, the distribution shows peaks at the angles predicted in this paper, namely $\pi/6, \pi/3, \pi/2 \dots$. In any way, to measure the forms of the carbon materials precisely, further developments may be needed in both hardware and software of the experimental technique. For example, to measure the kink angle of a kinked tube, one has to know the three dimensional configuration of the tube. It does not seem to be easily carried out by the present electron microscope technology, however it is not impossible in the future.

Next we discuss more theoretical aspect of the ar-

gument of this paper. It should be noted that we made some implicit assumption on the energetics of the graphitic carbon materials. For example, in Sec. 3.2 we have assumed that the cones are not elliptic cones but circular cones. This is because the latter seems to be more stable than the former from a natural intuition. We have also made similar assumptions in other arguments of this paper. If we argue these points more precisely, we have to calculate the elastic energy of the carbon materials. To do this we need to introduce a quantity which is not treated in this paper, that is the so-called *mean curvature* H (see Appendix A.2). As seen from the famous Gauss’s “*Theorem egregium (a most excellent theorem)*”, the Gaussian curvature is related only to the intrinsic properties of a surface. The word “intrinsic properties” means the properties that can be reached by measuring the lengths between arbitrary two points on the surface, namely, without looking from the outside of the surface. For a simple example, human beings before Gagarin could confirm the fact that the earth is round by just navigating all over the world. However, if the earth is cone-shaped, it is absolutely impossible to say whether the cone is a circular one or an elliptic one by only navigating on it, since they have the same intrinsic properties. This information can be obtained only by looking the surface from the outside. Looking from the outside is, actually, equivalent with measuring the mean curvature. Therefore the elastic energy of a carbon material should be related to the mean curvature. Some more efforts are needed to construct the theory which treats this problem. However we leave it for future studies. Here is one unsolved problem:

If there is a disclination with positive curvature in a graphite sheet, the surface forms a circular cone.

Then what if the curvature is negative?

The answer is not trivial but the situation like this may be possible in actual graphitic carbon materials. I hope someday such intriguing graphitic carbon materials are actually observed.

5. Summary

In this paper, we have applied the knowledge of differential geometry to the morphology of graphitic carbon materials. We have clarified how the quantization of the Gaussian curvature affects the forms of the graphitic carbon materials, such as spheres, cones, kinked tubes and structures with branches including Y-junctions. Especially it is predicted that the corner angle of a kinked nanotube is quantized by $\pi/6$. Experimental methods to observe these properties are also discussed.

Appendix A: Curvature

A.1 Curvature of a curve

First we begin with the definition of the curvature of a curve. As shown in Fig. 6 we parametrize curve C by a parameter s which is the length along C . Points on C is then written as $\vec{r}(s)$. Now consider two points on the curve indicated by A and B , the distance between which is ds (an infinitesimal number). The tangent vectors,

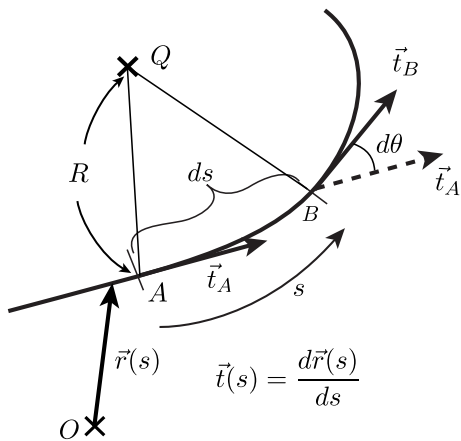


Fig. 6. Curve C , parametrized by the length s , and its tangent vectors \vec{t}_A and \vec{t}_B at points A and B , respectively. The distance between A and B is infinitesimal ds . The angle between \vec{t}_A and \vec{t}_B defines $d\theta$ and $|d\theta/ds|$ gives the curvature κ of C at A in the limit of $ds \rightarrow 0$. The center of the curvature is denoted by Q and R is the radius of the curvature.

given by $d\vec{r}/ds$, at A and B are denoted by \vec{t}_A and \vec{t}_B , respectively. We define $d\theta$ as the angle between \vec{t}_A and \vec{t}_B . Now the curvature κ of C is given by

$$\kappa = \left| \frac{d\theta}{ds} \right| = \left| \frac{d^2\vec{r}}{ds^2} \right|. \quad (\text{A}\cdot 1)$$

The center of curvature, denoted by Q in Fig. 6, is obtained by considering the curve AB as a part of a circle and finding the center of it. The radius of the circle R is called the radius of curvature and is related to the curvature κ by $\kappa = 1/R$.

In case of a plane curve, which is a curve included in a single plane, we can define κ by $d\theta/ds$ with a sign by appropriately choosing the direction $\theta = 0$. In this case, the integral of κ from a point A ($s = s_A$) to B ($s = s_B$) gives the angle made by the tangent lines of C at A and B ,

$$\int_{s_A}^{s_B} ds \kappa = \int_{s_A}^{s_B} ds \frac{d\theta}{ds} = \theta(s_B) - \theta(s_A). \quad (\text{A}\cdot 2)$$

A.2 Gaussian curvature of a surface

Next we describe the Gaussian curvature of a curved surface. As shown in Fig. 7(a), we consider the normal vector \vec{n} of the surface S at point A . Then consider a plane P which includes \vec{n} . The cross section of S and P defines a plane curve (dotted line). The curvature of this curve depends on the direction of P . If we rotate P around \vec{n} , the curvature changes and takes a maximum and a minimum before we rotate P by π . (Note that the curvature can be either positive or negative.) Let κ_1 and κ_2 be the maximum and the minimum of the curvature, respectively. Then the Gaussian curvature K at A is given by the product $\kappa_1\kappa_2$. Another curvature frequently used in the differential geometry is the mean curvature H defined by $(\kappa_1 + \kappa_2)/2$. At so-called *navel points* we find $\kappa_1 = \kappa_2$.

The Gaussian curvature can be either positive or negative. Surfaces with positive and negative Gaussian cur-

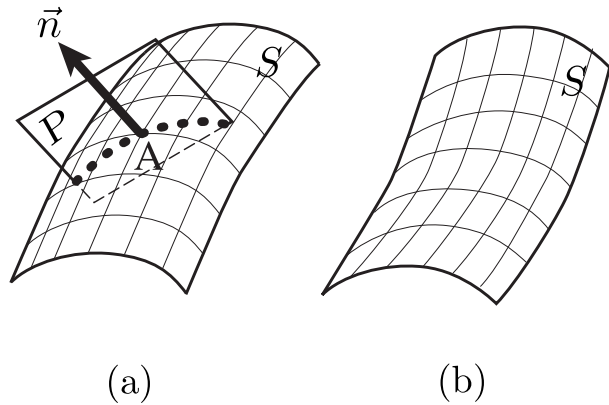


Fig. 7. (a) Surface S , its normal vector \vec{n} at point A and a plane P including \vec{n} . Cross section between A and P is shown by a dotted line. (b) A surface with negative Gaussian curvature.

vatures are depicted in Fig. 7(a) and (b), respectively.

A surface with vanishing Gaussian curvature is called a *developable surface*. If we cut off a piece of a developable surface, we can develop the piece on a plane without expanding or contracting any part of the piece. For example, sides of cylinders and cones are developable surfaces, but spheres are not.

Appendix B: Gauss-Bonnet theorem

B.1 Geodesic curvature

Before introducing the Gauss-Bonnet theorem, we describe the definition of the geodesic curvature and geodesic curves. Geodesic curvature is defined for a curve on a surface. In Fig. 8, we have shown a curve C on a surface S . Now consider a tangent plane of S at point A , which we denote by T in Fig. 8 (a). The point A is also on the curve C . Then consider the orthogonal projection of C onto T , which we denote by C_g . Geodesic curvature of the curve C at A is given by the curvature of the curve C_g at A . Let us denote it by κ_g . A curve on a surface whose geodesic curvature vanishes is called a geodesic curve. The sign of κ_g is determined by introducing the orientation of S . This point will be discussed later in relation to the Gauss-Bonnet theorem.

Next we consider a normal vector \vec{n} of the surface S at A and, then, consider a plane N which includes \vec{n} . The cross section between S and N defines a curve, which we denote by C_n . Here we set the direction of N so that C_n and C have a common tangent line at A . The curvature of C_n at A gives the normal curvature of C at A , which we denote by κ_n . Let the curvature of C at A be denoted by κ , then the following relation holds,

$$\kappa^2 = \kappa_n^2 + \kappa_g^2. \quad (\text{B}\cdot 1)$$

B.2 Gauss-Bonnet theorem

The Gauss-Bonnet theorem is expressed in several forms.

First we consider simply connected region D on a surface S surrounded by a smooth curve, denoted by C , as shown in Fig. 9 (a). The Gauss-Bonnet theorem is

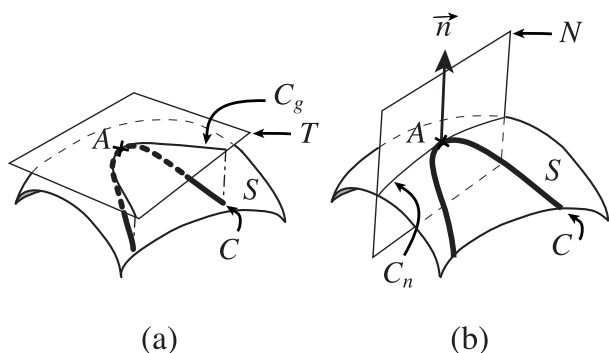


Fig. 8. C is a curve on a surface S . (a) The plane denoted by T is the tangent plane of S at a point A , where A is on C . The orthogonal projection of C onto T is C_g . The curvature of C_g at A gives geodesic curvature κ_g of C at A . (b) N is the normal plane of S at A , which is parallel to the normal vector \vec{n} of S at A . The cross section of S and N is a curve denoted by C_n . The curvature of C_n at A gives the normal curvature κ_n of C at A . Note that the direction of N is determined so that C_n and C have a common tangent line at A .

expressed as

$$\int_C \kappa_g ds + \iint_D K dA = 2\pi, \quad (\text{B}\cdot 2)$$

where κ_g is the geodesic curvature of C , and the second term is the integration of the Gaussian curvature K over D . Here the geodesic curvature is defined with a sign: we set $\kappa_g > 0$ ($\kappa_g < 0$) if the curve is convex (concave) viewing from the inside of D . This equation relates the total Gaussian curvature in the region D and the geodesic curvature of the boundary C .

If we consider a sectionally smooth curve with N vertices as shown in Fig. 9(b), the Gauss-Bonnet theorem reads,

$$\int_{C'} \kappa_g ds + \iint_D K dA = 2\pi - \sum_{i=1}^N \theta_i, \quad (\text{B}\cdot 3)$$

where C' means that the integral is evaluated except for the vertex points. θ_i is the exterior angles of the vertices, as shown in Fig. 9(b).

If we consider a geodesic polygon, which is a polygon with all the sides begin geodesic curves, the Eq. (B-3) is further reduced to

$$\iint_D K dA = 2\pi - \sum_{i=1}^N \theta_i, \quad (\text{B}\cdot 4)$$

since the geodesic curvature of the boundary vanishes.

If S is not a simply connected surface, the Gauss-Bonnet theorem has a more profound form. Here we limit ourselves to the case of the closed surfaces. Now, D covers the whole region of S . We obtain the following

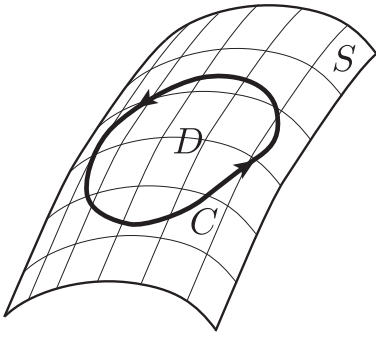
theorem,

$$\iint_S K dA = 2\pi\chi(S) = 4\pi(1 - g), \quad (\text{B}\cdot 5)$$

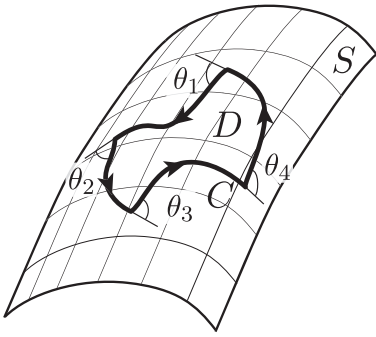
where $\chi(S)$ is the Euler characteristic of the surface, given by $\chi(S) = F - E + V$ where F , E and V are the number of faces, edges and vertices that occur in the

triangulation of the surface. Here g is the genus of the surface, *e.g.*, zero for a sphere, one for a torus. See, for example, Ref. 28 for more details.

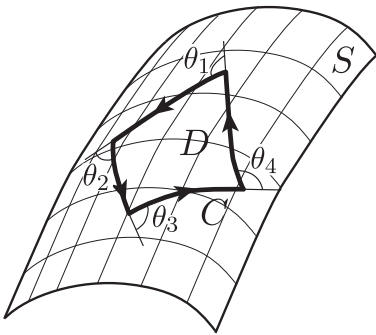
- 1) H. W. Kroto, J. R. Heath, S. C. O'Brien, R. F. Curl and R. E. Smalley, *Nature* **318** (1985) 162.
- 2) E. Osawa, *Kagaku* **25** (1970) 854 (in Japanese).
- 3) S. Iijima, *J. Phys. Chem.* **91** (1987) 3466.
- 4) R. F. Curl and R. E. Smally, *Science* **242** (1988) 1017.
- 5) H. W. Kroto, *Science* **242** (1988) 1139.
- 6) S. Iijima, *Nature* **354** (1991) 56.
- 7) H. W. Kroto, *Nature* **329** (1987) 529.
- 8) W. Krätschmer, L. D. Lamb, K. Fostiropoulos and D. R. Huffman, *Nature* **347** (1990) 354.
- 9) S. Iijima, T. Ichihashi and Y. Ando, *Nature* **356** (1992) 776.
- 10) S. Iijima and T. Ichihashi, *Nature* **363** (1993) 603.
- 11) Z. Yao, H. W. Ch. Postma, L. Balents and C. Dekker, *Nature* **402** (1999) 273.
- 12) B. C. Satishkumar, P. J. Thomas, A. Govindaraj and C. N. R. Rao, *Appl. Phys. Lett.* **77** (2000) 2530.
- 13) H. W. Kroto and K. McKay, *Nature* **331** (1988) 328.
- 14) A. L. McKay and H. Terrones, *Nature* **352** (1991) 762.
- 15) T. Lenosky, X. Gonze, M. Teter and V. Elser, *Nature* **355** (1992) 333.
- 16) G. Seifert, H. Terrones, M. Terrones, G. Jungnickel and T. Frauenheim, *Phys. Rev. Lett.* **85** (2000) 146.
- 17) S. Tanda, private communication.
- 18) S. Tanda, T. Tsuneta, Y. Okajima, K. Inagaki, K. Yamaya and N. Hatakenaka, *Nature* **417** (2002) 397.
- 19) In case of kinked tubes, it is not clear whether the region outside of the disclinations is really free from Gaussian curvature. However, for sufficiently large tubes as compared to the hexagons of the graphite sheet, it can be assumed that the Gaussian curvature is vanishingly small apart from the disclinations.
- 20) There may be some correction arising from the change of κ . We found that this is the same order as that from κ_n . This point will be discussed elsewhere.
- 21) A. N. Andriotis, M. Menon, D. Srivastava and L. Chernozatonskii, *Phys. Rev. Lett.* **87** (2001) 066802-1.
- 22) R. Martel, H. R. Shea and P. Avouris, *Phys. Chem.* **36** (1999) 7551.
- 23) M. B. Nardelli and J. Bernholc, *Phys. Rev. B* **60** (1999) R16338.
- 24) Y. Shibata and S. Maruyama, *Physica B* **323** (2002) 187.
- 25) M. Terrones, F. Banhart, N. Grobert, J.-C. Charlier, H. Terrones and P. M. Ajayan, *Phys. Rev. Lett.* **89** (2002) 075505.
- 26) L.-M. Peng, Z. L. Zhang, Z. Q. Xue, Q. D. Wu, Z. N. Gu and D. G. Pettifor, *Phys. Rev. Lett.* **85** (2000) 3249.
- 27) Y. Zhao, R. E. Smally and B. I. Yakobson, *Phys. Rev. B* **66** (2002) 195409.
- 28) D. J. Struik, *Lectures on Classical Differential Geometry* (Addison-Wesley, 1950, Massachusetts).



(a)



(b)



(c)

Fig. 9. (a) A smooth curve C , (b) a sectionally smooth curve C with several vertices, and (c) a polygon C whose sides are geodesic curves on the surface S . D is the region surrounded by C .